S. Guizani, A. Nayli, F. Ben Ammar

## Fault-tolerant control of a double star induction machine operating in active redundancy

Introduction. The operating safety of a variable-speed drive is of paramount importance in industrial sectors, such as electric propulsion for ships, rail transport, electric cars, and aircraft, where reliability, maintainability, and safety are top priorities. Problem. One solution to improve the availability of a variable-speed drive is the use of a double star induction machine (DSIM). This machine can provide active or passive redundancy. Redundancy is active if both converters operate simultaneously, and the failure of one of them does not affect system operation. Passive redundancy is passive if only one converter is operating and the 2nd is on standby; the latter will only operate if the first fails. Goal. Improving the availability of a DSIM by the operation in active redundant of the machine supply system. Methodology. Use scalar control to control the machine power system in active redundancy. Simulation results with this scalar control demonstrated the need to equip this control with a decoupling of the variables responsible for machine magnetization and torque production. Field-oriented control (FOC) is then used to ensure the reconnection of a converter after a failure for active redundancy operation, without the risk of significant torque ripples. Scientific novelty. To increase the availability of the variable speed drive, an original control strategy for reintegrating the repaired faulty inverter is implemented to allow the repaired inverter to resume operation of the drive motor. This strategy control is based on the specific use of FOC to resynchronize the output frequency of the repaired inverter with the motor speed. Results. The results demonstrated the value of vector control in each star power supply system to avoid transient over currents at the input of the 2nd converter, by synchronizing the frequency of the 2 converters to the rotor speed. Practical value. An experimental model around a DSIM is set up to validate the active redundancy operation of the system. Active redundancy provides the variable speed drive with an increase in the reliability of the variable speed drive and significantly improves the availability rate of the driven load, since the disconnection of one of the 2 converters following a failure does not affect the operation of the machine. References 17, tables 2, figures 13. Key words: double star induction machine, active redundancy, field-oriented control, reliability.

Вступ. Безпека експлуатації частотно-регульованого приводу має першорядне значення в таких галузях промисловості, як електроприводи для суден, залізничного транспорту, електромобілів та літаків, де надійність, ремонтопридатність та безпека  $\epsilon$  головними пріоритетами. **Проблема**. Одним із рішень для підвищення готовності частотно-регульованого приводу  $\epsilon$ використання асинхронного двигуна з подвійною зіркою (DSIM). Цей двигун може забезпечувати активне чи пасивне резервування. Резервування активно, якщо обидва перетворювачі працюють одночасно, і відмова одного з них не впливає на роботу системи. Пасивне резервування пасивне, якщо працює лише один перетворювач, а другий перебуває у резерві; останній працюватиме лише у разі відмови першого. **Мета**. Підвищення готовності DSIM завдяки роботі в режимі активного резервування системи живлення машини. Методика. Використання скалярного керування для управління системою живлення машини в режимі активного резервування. Результати моделювання з використанням скалярного управління показали необхідність оснашення управління поділом змінних, що відповідають за намагнічування машини та створення крутного моменту. Далі використовується полеорієнтоване управління (FOC) для забезпечення повторного підключення перетворювача після відмови для роботи в режимі активного резервування без ризику значних пульсацій крутного моменту. Наукова новизна. Для підвищення готовності перетворювача частоти реалізовано оригінальну стратегію управління для повторного підключення відремонтованого несправного перетворювача, що дозволяє відремонтованому перетворювачу відновити роботу приводного двигуна. Ця стратегія управління заснована на специфічному використанні FOC для повторної синхронізації вихідної частоти відремонтованого перетворювача зі швидкістю двигуна. Результати продемонстрували цінність векторного управління в кожній зіркоподібній системі електропостачання для запобігання перехідним струмам на вході другого перетворювача шляхом синхронізації частоти двох перетворювачів зі швидкістю ротора. Практична цінність. Створено експериментальну модель на основі DSIM для перевірки роботи системи в режимі активного резервування. Активне резервування забезпечує підвищення надійності перетворювача частоти і значно покращує коефіцієнт готовності навантаження, оскільки відключення одного з двох перетворювачів після відмови не впливає на роботу машини. Бібл. 17, табл. 2, рис. 13.

Ключові слова: асинхронна машина з подвійною зіркою, активне резервування, полеорієнтоване управління, надійність.

Introduction. In the speed drive applications (pumps, fans, extruders, railway traction, drive of the compressors in the methane tankers, electric propulsion of the ships etc.) [1–3], the use of multiphase or multi-stars asynchronous machine offers multiple redundancy degrees [4–6], since the loss of one star does not stop the machine. For motors and drives for surface ship propulsion, particular attention is paid to the separation of the phases, motor and inverter connection scheme [7]. As consequence of complete separation between the phases, the loss of any motor or inverter phase will not jeopardize the remaining phases and continue operation at reduced load.

In the case of 6 phase induction machine, different configurations are possible. In Fig. 1,*a* the stator can be realized with a single star point with a 6 independent armature currents [8, 9]. As shown in Fig. 1,*b*, to avoid the 3rd harmonics, the 6 stator windings can be combined into 2 three phase windings; the star points are kept isolated with 2 pairs of independent stator currents.

In the asymmetrical stator windings structure the 2 three phase windings are spatially shifted by 30°.

The symmetrical winding structure with displacement between any 2 consecutive stator phases is

60° [10, 11]. It's shown by that non shifted star windings are preferred to have a weak magnetic coupling between stars. Figure 1,c shows the configuration in which each phase is electrically insulated from the others for independent control; each phase is supplied with H-bridge voltage source inverter (VSI). In Fig. 1,d the 2 stator windings are not mutually coupled, this aim can be accomplished if the 2 stator windings are designed with a different number of poles.

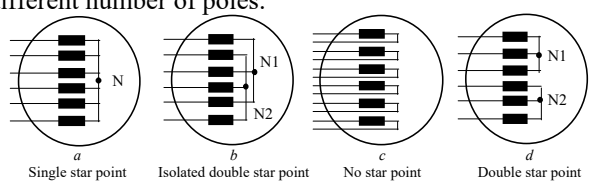
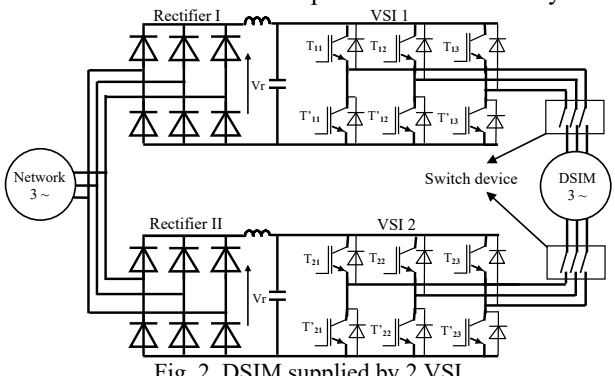


Fig. 1. Six phases induction machine

As shown in Fig. 2, the drive-motor configuration employs 2 identical pulse-width modulation VSIs to supply the double star induction machine (DSIM) [12–14]. The failure that may involve VSI can take place either in the diodes of the rectifier, in the DC link capacitors and the switches of the inverter or in their gate control circuit.

© S. Guizani, A. Nayli, F. Ben Ammar

Note that the reliability level is increased if the IGBT driver uses differential signal processing to provide a high level of signal integrity and high noise rejection. For example, with the over voltages, especially those that occur during a short-circuit turn-off, are reduced by the IGBT driver like Skyper 52 of Semikron, using intelligent turn-off control to switch the power transistor slowly.



To detect the failure inverter, the controller receives feedback from each gate drive IGBT signals. If the fault is detected, then the inverter can be disconnected and electrically isolated from the corresponding star stator winding while continuing to operate using the healthy inverter. In case of failure in one inverter the motor will be driven with up to half of maximal torque. The faulty inverter can be repaired or replaced and reintegrated into the system without over-voltage or over-current.

The **goal** of this work is to improve the availability of a DSIM by the operation in active redundant of the machine supply system.

The scalar control. Figure 3 shows the simulation for a load torque of the form  $T_r = kn$ . We considered the disconnection of converter 2 following a failure, then its reintegration into the machine power supply.

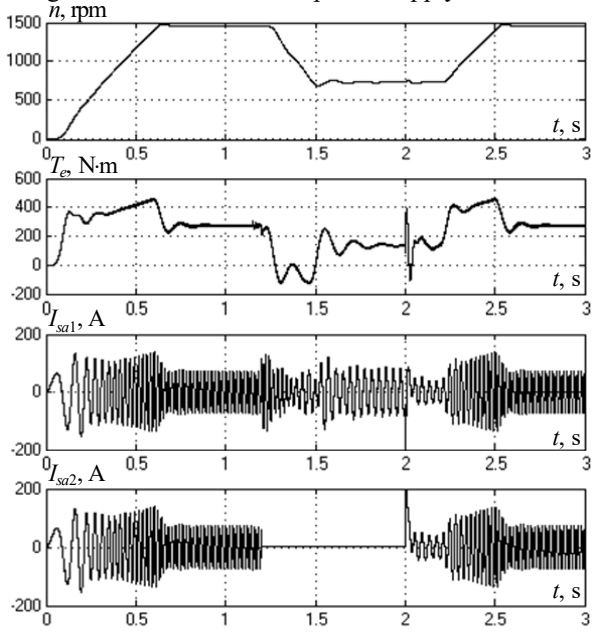


Fig. 3. Simulation of the converter 2 reconnection after the power supply failure of star 2 for a load torque  $T_r = kn$ 

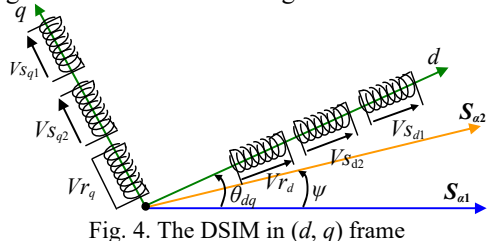
The operation consists of a start cycle between t = 0 and t = 0.6 s. At t = 1.2 s we disconnected converter 2 supplying the 2nd star following a failure. The speed is then reduced to 50 % of the nominal speed. At time t = 2.5 s, we simulated the reconnection of converter 2.

The parameters of DSIM are:  $R_r$ ,  $R_s$  are the rotor and stator resistances;  $M_{ss}$  is the mutual inductance between 2 stars of the stator;  $M_{sr1}$  is the mutual cyclic inductance between star 1 and rotor;  $M_{sr2}$  is the mutual cyclic inductance between star 2 and rotor;  $L_s$ ,  $L_r$  are the stator and rotor cyclic inductances;  $T_e$  is the electromagnetic torque;  $T_L$  is the load torque; p is the number of pole pairs.

Preliminary results have shown significant ripples in the torque and stator currents during the reconnection of the 2nd star. Scalar redundancy therefore does not allow for the reintegration of the repaired converter.

To increase the availability of the variable speed drive, an **original control strategy** for reintegrating the repaired faulty inverter is implemented to allow the repaired inverter to resume operation of the drive motor. This strategy control is based on the specific use of field-oriented control (FOC) to resynchronize the output frequency of the repaired inverter with the motor speed.

The model obtained by using Park's transformation (Fig. 4) is undoubtedly the best adapted for the description of the DSIM behavior at the transient, as well as steady state operation [14–16]. The control strategy and fault manager software of the double stator supplied by redundant VSIs are realized in the field rotating (d, q) orthogonal axes reference frame running at  $\omega_{dq}$ . The decoupling between the torque and the flux are be accomplished by properly aligning the rotor flux vector along the d-axis.



1 ig. 4. The DShvi in (a, q) frame

The mathematical flux model is written in (d, q) reference frame, and described as:

$$\begin{cases} \frac{\mathrm{d}X(t)}{\mathrm{d}t} = \left[A(\omega, \omega_{dq})\right] [X(t)] + [B]U(t); \\ Y(t) = [C]X(t), \end{cases}$$
 (1)

where  $X(t) = [\Phi_{sd1}, \Phi_{sq1}, \Phi_{sq2}, \Phi_{sd2}, \Phi_{rd}, \Phi_{rq}]^t$  is the state vector;  $U(t) = [U_1, U_2]^t = [V_{sd1}, V_{sq1}, V_{sd2}, V_{sq2}]^t$  is the control vector;  $Y(t) = [I_{sd1}, I_{sq1}, I_{sd2}, I_{sq2}]^t$  is the output vector;  $\Phi_{rd}, \Phi_{rq}$  are the direct and orthogonal components of the rotor flux;  $I_{sd1}, I_{sq1}, I_{sd2}, I_{sq2}$  are the direct and orthogonal components of star 1 and star 2 current;  $\Phi_{sd1}, \Phi_{sq1}, \Phi_{sd2}, \Phi_{sq2}$  are the direct and orthogonal components of star 1 and star 2 flux;  $V_{sd1}, V_{sq1}, V_{sd2}, V_{sq2}$  are the direct and orthogonal components of star 1 and star 2 voltages;  $\psi$  is the shifting angle between 2 stars of the stator;  $\theta_{dq}$  is the displacement between d-axis and the  $\alpha_1$ -axis of the star 1 of the stator;  $\theta_{dq} - \psi$  is the displacement between d-axis and the  $\alpha_2$ -axis of the star 2 of the stator;  $\theta_{dq} - \theta$  is the displacement between d-axis and the  $\alpha_2$ -axis of the rotor.

The state matrix is determined as:

$$[A(\omega, \omega_{dq})] = -([R][L_{d,q}]^{-1} + [W]); \qquad (2)$$

$$[C] = [L_{d,q}]^{-1}; \qquad (3)$$

$$\begin{bmatrix} L_s & 0 & M_{ss} & 0 & M_{sr1} & 0\\ 0 & L_s & 0 & M_{ss} & 0 & M_{sr1}\\ M_{ss} & 0 & L_s & 0 & M_{sr2} & 0\\ 0 & M_{ss} & 0 & L_s & 0 & M_{sr2}\\ M_{sr1} & 0 & M_{sr2} & 0 & L_r & 0\\ 0 & M_{sr1} & 0 & M_{sr2} & 0 & L_r \end{bmatrix}. (4)$$

In case of failure in VSI 1, it could be disconnected from star 1 of stator winding. In the inductance matrix  $[L_{d,q}]_{f1}$  the terms involving  $M_{sr1}$  and  $M_{ss}$  can be ignored.

Similarly, in the inductance matrix  $[L_{d,q}]_{f2}$  the terms involving  $M_{sr2}$  and  $M_{ss}$  can be ignored in case of the disconnection of star 2 stator winding:

Fig. 5. The block diagram of DSIM with FOC strategy

The feedback regulators are working in coordinates which rotates synchronously with the rotor flux in all operating modes; the direction of axis d is always coincident with the rotor flux representative vector. The

measurements stators current are transformed to field-oriented quantities  $I_{sd1}$ ,  $I_{sq1}$  and  $I_{sd2}$ ,  $I_{sq2}$ . In a large speed range, rotor flux  $\Phi_{rd}$  is kept at constant nominal values controlling direct axis currents  $i_{sd1}$  and/or  $i_{sd2}$ .

Table 1 shows speed and rotor flux references in different operating inverter states.

Speed and rotor flux references in different operating

Speed and rotor flux references in different operating		
State of motor drive	Speed reference	Rotor flux references
Inverter 1 up Inverter 2 up	$\omega_{refl} = \omega_n \ \omega_{ref2} = \omega_n$	$ \Phi_{rdref1} = \Phi_n/2 $ $ \Phi_{rdref2} = \Phi_n/2 $
Inverter 1 up Inverter 2 down	$\omega_{ref} = \omega_n/2$ if $T_L = k\omega$ $\omega_{ref} = \omega_n/\sqrt{2}$ if $T_L = k\omega^2$	<i>A A</i>
Inverter 1 down Inverter 2 up	$\omega_{ref} = \omega_n/2$ if $T_L = k\omega$ $\omega_{ref} = \omega_n/\sqrt{2}$ if $T_L = k\omega^2$	$ \Phi_{rdref2} = \Phi_n $
Inverter 1 down Inverter 2 down	0	0

Table 2 shows the electromagnetic torque, the speed of rotor flux vector and the magnitude of rotor flux in all operating configurations.

Table 2 Electromagnetic torque and rotor flux in (d, q) plane aligned with the rotor flux in 4 operating inverters states

	1 0	
State of motor	Electromagnetic torque $T_e$ ;	Rotor flux $\Phi_{rd}(p)$
drive	Field speed $\omega_{dq}$	
Inverter 1 up Inverter 2 up	$\begin{split} T_e &= \frac{3M_{sr}p \varPhi_{rd}}{2L_r} \Big(I_{sq1} + I_{sq2}\Big) \\ \omega_{dq} &= \omega + \frac{M_{sr}}{T_r \varPhi_{rd}} \Big(I_{sq1} + I_{sq2}\Big) \end{split}$	$\frac{M_{sr1}}{1+T_rp} \left( I_{sd1} + I_{sq2} \right) (p)$
	$T_r \Phi_{rd}$	
Inverter 1 up Inverter 2 down	$T_e = \frac{3M_{sr1}p\Phi_{rd}}{2L_r}I_{sq1}$ $\omega_{dq} = \omega + \frac{M_{sr}}{T\Phi_{rd}}I_{sq1}$	$\frac{M_{sr1}}{1+T_rp}I_{sd1}(p)$
Inverter 1 down Inverter 2 up	$T_r \Phi_{rd}$ $T_e = \frac{3M_{sr2} p \Phi_{rd}}{2L_r} I_{sq2}$ $\omega_{dq} = \omega + \frac{M_{sr}}{T_r \Phi_{rd}} I_{sq2}$	$\frac{M_{sr2}}{1+T_rp}I_{sd2}(p)$
Inverter 1 down Inverter 2 down	0	0

The results simulation (Fig. 6) shows the active redundancy operation of the system using the reconfiguration and reintegration control strategy of the repaired inverter is based on the special use of the FOC [14–16]. The operating description is as follows:

- 1) for  $0 \le t < 0.2$  s: machine fluxing provided by the 2 currents  $I_{sd1}$ ,  $I_{sd2}$  the reference fluxes are  $\Phi_{rdref1} = \Phi_{rdref2} = 0.5 \Phi_n$ .
- 2) for  $0.2 \le t < 0.8$  s: acceleration from 0 to 1460 rpm.
- 3) for  $0.8 \le t < 1.49$  s: machine operation at nominal speed.
- 4) at t = 1.49 s: fault in converter 2.

DSIM

- 5) for  $1.49 \le t < 1.59$  s: the current  $I_{sd1}$  of the healthy star winding is controlled to impose the required rotor flux. The motor must be controlled at half speed.
- 6) for  $1.59 \le t < 2.1$  s: deceleration from 1460 to 730 rpm.
- 7) for  $2.48 \le t < 3.1$  s: once the faulty converter is replaced or repaired, it will attempt to return to normal operation. The prerequisite for the repaired converter to return to a healthy state is for the output frequency to be resynchronized with the motor speed.
- 8) for  $t \ge 3.1$  s: machine operation at nominal speed.

In active redundancy operation, the converters are sized for a power 0.5*P*. Thus, in degraded mode, the speed

is reduced to 50 % or 70 % of the nominal speed depending on whether the torque is in the form of kn or  $kn^2$ .

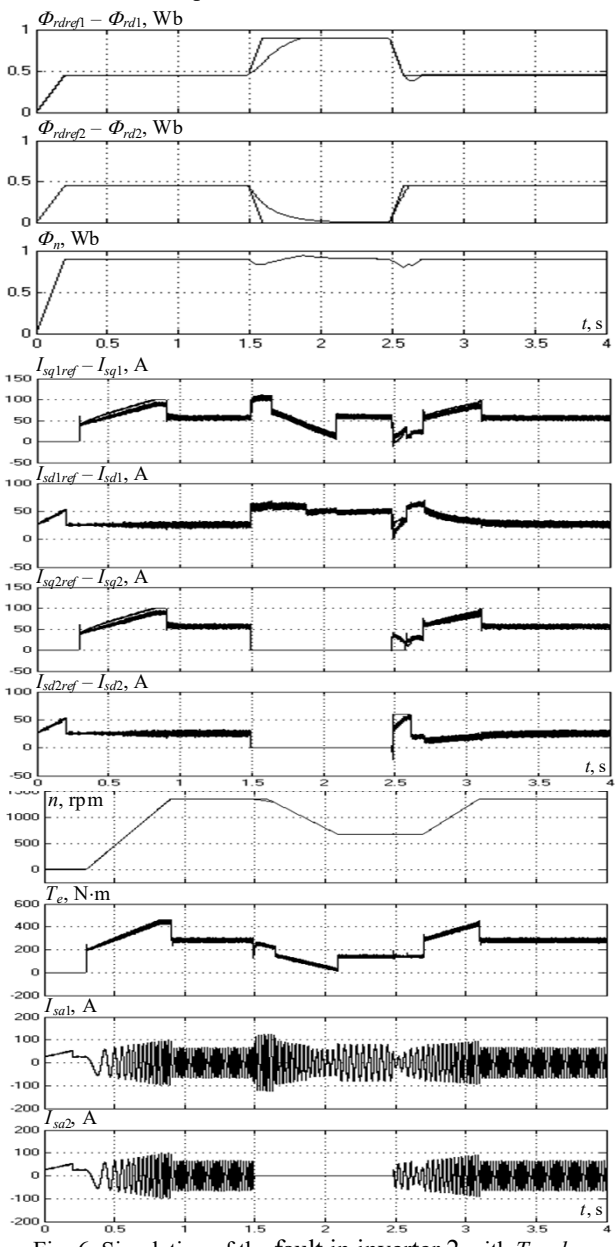


Fig. 6. Simulation of the fault in inverter 2 with  $T_r = kn$ 

**Experimental results.** In Fig. 7 the experimental platform shows the DSIM shifted by 30 el. degrees of 1.5 kW power feeding by 2 VSI using Spartan 3E FPGA board [17].

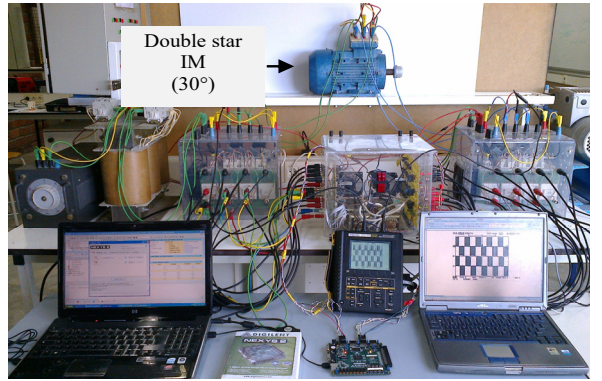


Fig. 7. Experimental platform

The obtained experimental results of the active redundant operating mode of supply system of the DSIM

are shown in Fig. 8–13. The voltage between 2 phases of the 1st and the 2nd star before and after fails and after reintegration of inverter 2 are shown in Fig. 8.

The voltage between 2 phases of the 1st star and stator current in the 2nd star after fails and after reintegrated of inverter 2 are given in Fig. 9.

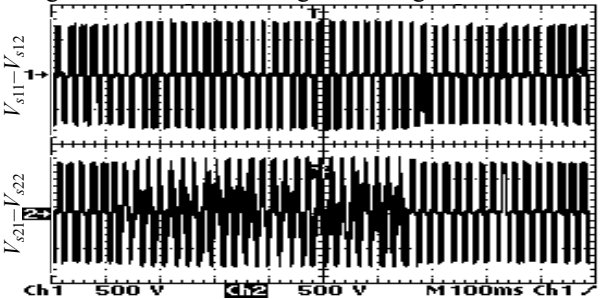


Fig. 8. Voltage between 2 phases of the 1st star and the 2nd star before and after fails and after reintegration of inverter 2

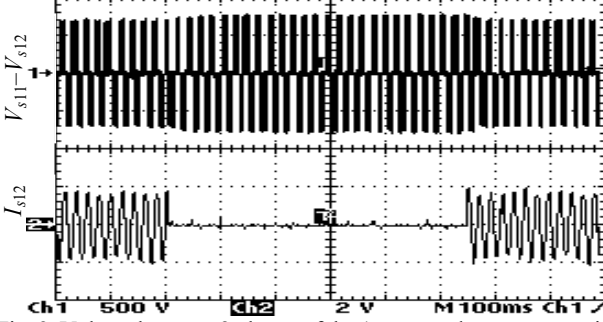


Fig. 9. Voltage between 2 phases of the 1st star and stator current in the 2nd star before and after fails and after reintegration of inverter 2

The voltage between 2 phases of the 1st star and stator current in the 2nd star after fails and after reintegrated of inverter 2 are shown respectively in Fig. 10, 11.

The voltage between 2 phases and stator current in the 2nd stator after fails of inverter 2 are given in Fig. 12.

The voltage between 2 phases and stator current in the 2nd stator after reintegrated of inverter 2 are given in Fig. 13.

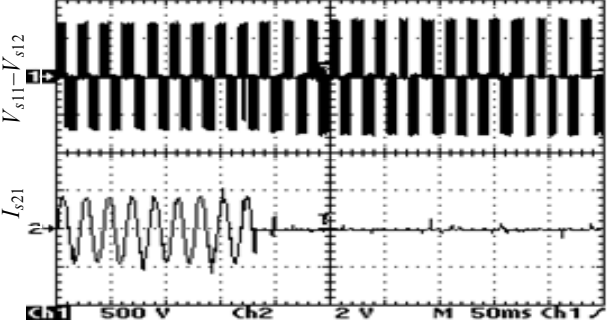


Fig. 10. Voltage between 2 phases of the 1st star and stator current in the 2nd stator before and after fails

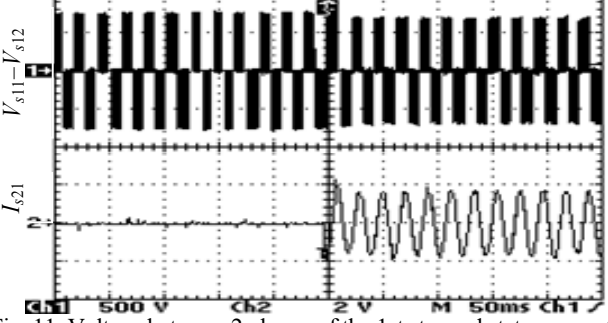


Fig. 11. Voltage between 2 phases of the 1st star and stator current in the 2nd stator before and after reintegrated of inverter 2

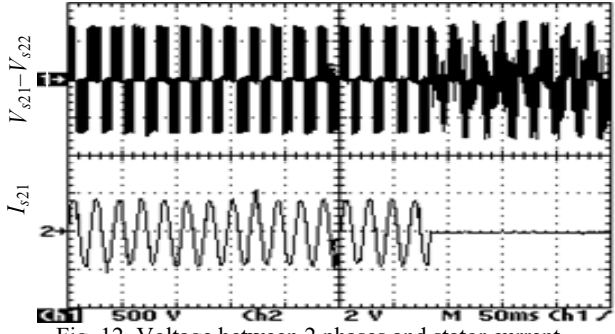
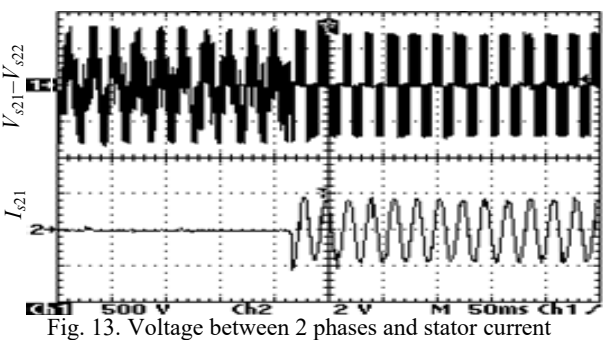


Fig. 12. Voltage between 2 phases and stator current in the 2nd stator before and after fails of inverter 2



in the 2nd stator before and after reintegrated of inverter 2

**Conclusions**. The aim of this work was the DSIM supplied by redundant VSIs improves reliability, availability and safety of the system since the loss of a one star does not stop the motor. A control strategy by reintegration of the repaired faulty inverter increases system survivability by allowing the faulty inverter to resume operation of the drive motor. The 1st strategy based on scalar control demonstrated its weaknesses in terms of torque and stator current during converter reintegration. To address these weaknesses, the 2nd strategy was used. This reintegration control strategy relies on the specific use of FOC to resynchronize the output frequency of the repaired inverter with the motor speed. Simulation results of FOC of the active redundancy operation of the DSIM power supply demonstrated a good solution for fault-tolerant control. Indeed, the reintegration of repaired inverter gave for the 1st control strategy a current peak of 200 A (maximum value) whereas with the faulttolerant control strategy, the current gradually goes from 0 to 100 A (maximum value), then it stabilizes at its nominal value. This is also true for the torque.

Experimental results on a 1.5 kW DSIM are performed to demonstrate the ability of a fault-tolerant architecture to improve availability.

Conflict of interest. The authors declare that they have no conflicts of interest.

## REFERENCES

- 1. Nemouchi B., Rezgui S.E., Benalla H., Nebti K. Fractional-based iterative learning-optimal model predictive control of speed induction motor regulation for electric vehicles application. Electrical Engineering & Electromechanics, 2024, no. 5, pp. 14-19. doi: https://doi.org/10.20998/2074-272X.2024.5.02.
   Chaib Ras A., Bouzerara R., Bouzeria H. An adaptive controller for
- power quality control in high speed railway with electric locomotives with asynchronous traction motors. Electrical Engineering & *Electromechanics*, 2024, no. 2, https://doi.org/10.20998/2074-272X.2024.2.04. pp.
- 3. Khemis A., Boutabba T., Drid S. Model reference adaptive system speed estimator based on type-1 and type-2 fuzzy logic sensorless control of electrical vehicle with electrical differential. Electrical

Engineering & Electromechanics, 2023, no. 4, pp. 19-25. doi: https://doi.org/10.20998/2074-272X.2023.4.03.

- 4. Guizani S., Nayli A., Ben Ammar F. Comparison between star winding and open-end winding induction machines. *Electrical* Engineering, 2016, vol. 98, no. https://doi.org/10.1007/s00202-016-0359-4. 219-232. no. 3, pp.
- 5. Sun J., Zheng Z., Li C., Wang K., Li Y. Optimal Fault-Tolerant Control of Multiphase Drives Under Open-Phase/Open-Switch Faults Based on DC Current Injection. IEEE Transactions on Power Electronics, 2022, vol. 37, no. 5, https://doi.org/10.1109/TPEL.2021.3135280. pp. 5928-5936. doi:
- Letellier P. Electrical propulsion motors. Electric Propulsion. The Effective Solution. Paper 7. London, IMarE, 1995.
- Mitcham A.J., Cullen J.J.A. Motors and drives for surface ship propulsion: comparison of technologies. Proceeding of 1995 Electric Propulsion Conference, 1995, vol. 4, pp. 88-89.
- 8. Abdel-Khalik A.S., Masoud M.I., Williams B.W. Vector controlled multiphase induction machine: Harmonic injection using optimized constant gains. Electric Power Systems Research, 2012, vol. 89, pp. 116-128. doi: <a href="https://doi.org/10.1016/j.epsr.2012.03.001">https://doi.org/10.1016/j.epsr.2012.03.001</a>.
- Abdelwanis M.I., Zaky A.A. Maximum power point tracking in a perovskite solar pumping system with a six-phase induction motor. Revue Roumaine des Sciences Techniques — Série Électrotechnique et 2024, vol. 69, no. 1. Énergétique, pp. 15-20. https://doi.org/10.59277/RRST-EE.2024.1.3.
- 10. Lim C.S., Lee S.S., Levi E. Continuous-Control-Set Model Predictive Current Control of Asymmetrical Six- Phase Drives Considering System Nonidealities. IEEE Transactions on Industrial 2023, vol. 70, no. 8, pp. 7615-7626. Electronics, https://doi.org/10.1109/TIE.2022.3206703.
- 11. Hammad R., Dabour S.M., Rashad E.M. Asymmetrical six-phase induction motor drives based on Z-source inverters: Modulation, design, fault detection and tolerance. Alexandria Engineering Journal, 2022, 61, no. 12, pp. 10055-10070. https://doi.org/10.1016/j.aej.2022.02.058.
- 12. Boukhalfa G., Belkacem S., Chikhi A., Benaggoune S. Genetic algorithm and particle swarm optimization tuned fuzzy PID controller on direct torque control of dual star induction motor. Journal of Central South University, 2019, vol. 26, no. https://doi.org/10.1007/s11771-019-4142-3. 7, pp. 1886-1896. doi:
- 13. Chaabane H., Khodja D.E., Chakroune S., Hadji D. Model reference adaptive backstepping control of double star induction machine with extended Kalman sensorless control. *Electrical Engineering & Electromechanics*, 2022, no. 4, pp. 3-11. doi: https://doi.org/10.20998/2074-272X.2022.4.01.
- 14. Zemmit A., Messalti S., Herizi A. New Direct Torque Control of Dual Star Induction Motor using Grey Wolf Optimization Technique. Przegląd Elektrotechniczny, 2024, no. 2, pp. 109-113. doi: https://doi.org/10.15199/48.2024.02.21
- 15. Abdelwanis M.I., Zaky A.A., Selim F. Direct torque control for a six phase induction motor using a fuzzy based and sliding mode controller. *Scientific Reports*, 2025, vol. 15, no. 1, art. no. 14874. doi: https://doi.org/10.1038/s41598-025-97479-1.
- 16. Moussaoui L. Performance enhancement of direct torque control induction motor drive using space vector modulation strategy. Electrical Engineering & Electromechanics, 2022, no. 1, pp. 29-37. doi: https://doi.org/10.20998/2074-272X.2022.1.04.
- 17. Aib A., Khodja D.E., Chakroune S., Rahali H. Fuzzy current analysis-based fault diagnostic of induction motor using hardware cosimulation with field programmable gate array. Electrical Engineering Electromechanics, 2023, 3-9. no. 6. pp. https://doi.org/10.20998/2074-272X.2023.6.01.

Received 11.05.2025 Accepted 16.07.2025 Published 02.11.2025

- S. Guizani<sup>1</sup>, Professor of Electrical Engineering,
- A. Nayli<sup>2</sup>, Doctor of Electrical Engineering,
- F. Ben Ammar<sup>3</sup>, Professor of Electrical Engineering,
- <sup>1</sup> University of El Manar, IPEIEM, Tunisia.
- <sup>2</sup>University of Gafsa, IPEIG, Tunisia,
- e-mail: abdelmonoem.nayli@gmail.com (Corresponding Author)
- MMA Laboratory, INSAT, University of Carthage, Tunisia.

How to cite this article:

Guizani S., Nayli A., Ben Ammar F. Fault-tolerant control of a double star induction machine operating in active redundancy. Electrical Engineering & Electromechanics, 2025, no. 6, pp. 27-31. doi: https://doi.org/10.20998/2074-272X.2025.6.04